A Numerical Study of the Role of Cold Convective Cloud Parameterization in Precipitation Pattern at Ground Surface

Sohaila Javanmard (Corresponding author)

Atmospheric Science and Meteorological Research Center (ASMERC), I. R. of Iran Meteorological Organization (IRIMO), Tehran 14965-114, I. R. of Iran

Tel: 98-21-2610-8094 E-mail: sohailajavanmard@gmail.com

Mahla Karim Pirhayati

Department of Physics, Zanjan University, Zanjan, Iran

Received: August 9, 2011 Accepted: August 22, 2011 Published: March 1, 2012

doi:10.5539/jgg.v4n1p269 URL: http://dx.doi.org/10.5539/jgg.v4n1p269

Abstract

In this paper, improvement of the one-dimensional cold thunderstorm model in view of microphysical parameterization has been presented. We included 32 microphysical processes with six water substances including water vapor, cloud droplet, cloud ice ,rain, snow, and hail (graupel) instead of nine cloud microphysical processes with four water substances (water vapor, cloud droplet, rain, and hail) . The developed cloud model showed a significant effect on the precipitation amount and pattern at the ground surface. The maximum rainfall intensity at the surface reached 114 mm/h instead of 34 mm/h. The time period of precipitation became 63 minutes instead of 51 minutes, i. e. it was reduced about 12 minutes. It can be said that the findings of the present study are more reasonable and consistent with the observed thunderstorm precipitation which produces high rainfall intensity naturally in a short period of time at the surface.

Keywords: Cloud model, Precipitation, Cold cloud, Parameterization, Microphysics processes

1. Introduction

Convective clouds are important in large-scale weather systems and climate modification. They are vital energy sources and regulators for wind systems on many scales (Simpson, 1970). These clouds play an important role in global precipitation and are main source of precipitation in tropical regions. In general, these clouds produce heavy rainfall in a short time. Therefore, prediction of such a process, quantitatively and qualitatively, could be studied in the cloud model only if microphysical processes are properly included. Ogura and Takahashi (1971) were the first to study this problem by coupled one-dimensional numerical model with bulk parameterization and were successful in discovering many dynamic and thermodynamic properties of thunderstorms by numerical modeling. They also showed the life cycle of thunder clouds through microphysics. Many other researchers have studied microphysical effects by using cloud modeling, for example Danielson *et al*. (1972), Koenig and Murray (1976), Lin *et al*. (1983), Javanmard (1995), Takahashi and Kawano (1997).

In Ogura and Takahashi model, nine cloud microphysical processes have been parameterized with four water substances including water vapor, cloud droplet, raindrop and hail. Javanmard and Jamali (2003) and Jamali and Javanmard (2004) have improved the microphysical parameterization in the Ogura and Takahashi model. The most important features of the Developed Ogura and Takahashi model (DOT) could be defined as the inclusion of Kessler parameterization concepts in a warm rain process, Bigg's freezing and terminal velocities of rain water and hail particles. On the other hand, Lin *et al*. (1983) created a two-dimensional, time-dependent cloud model with bulk parameterization. In this model, 32 microphysical processes were parameterized with six water substances including water vapor, cloud droplet, cloud ice, raindrop, snow and hail. In this research, in order to achieve more accurate prediction of precipitation including liquid and solid from convective clouds, we present the developed one-dimensional cloud model whose microphysical parameterization is based on the Lin *et al*., and its dynamical equations is based on DOT (Developed Lin *et al*. Microphysical Processes (DLMP)) (Rajaei, 2008; Javanmard *et al*., 2008). This model can be applied for more accurate prediction of spatial and temporal distribution of mixing ratios of cloud droplet, cloud ice, raindrop, snow, hail, and rainfall intensity profile at

ground. In this paper, the structure of numerical cloud models will be described in section 2. Then, the dynamical and microphysical structures of DOT, Lin *et al*., and DLMP models will be introduced. In section 3, the numerical procedure will be explained and in the last section, DOT and DLMP models outputs, including mixing ratios of raindrop (Q_r), hail (Q_G), snow (Q_s), rainfall intensity (PR), temperature difference between cloud and environment (TT), vertical velocity (w), and rainfall intensity at ground surface (GPR) will be compared.

2. Numerical Modeling of Microphysical and Dynamical Processes of Cloud

The numerical models are classified as zero dimensional (0D), one dimensional (1D), two dimensional (2D), and three dimensional (3D). In 0D models, complicated microphysical processes could be simulated well and they are suitable for prediction of the beginning of precipitation. 1D models include time-dependent (1DT) and steady-state (1DS) models. In 1DS models, dynamic and thermodynamic equations are considered only along the vertical axis but in 1DT models, time is added as an independent variable to 1DS. The models could also be coupled and uncoupled. In the coupled models, the microphysical variables depend on dynamic and thermodynamic parameters and they are independent in uncoupled models. In some one-dimensional models (1DS, 1DT), the microphysical parameterization is bulk and in others, microphysical details are considered. 1D models (1DS, 1DT) can predict cloud top height and cloud thickness changing before and after seeding, their execution time on computer is short, and they are applied in studying precipitation processes and operational cloud seeding experiments.

The majority of 2D models are bulk and they can simulate precipitation processes in a coupled framework and precipitation in updraft airflow. They are able to predict rainfall amount and location, and estimate optimum location and time of agent seeding dispersing. 2D models aren't complete in simulation and their dynamic and microphysics are simple. 3D models are complicated and their execution time on PC is long. These models could not be applied for operational purposes (Orville, 1996; Javanmard, 2003).

2.1 Developed Ogura and Takahashi (DOT) Model

Developed Ogura and Takahashi (DOT) model is a time-dependent and one-dimensional model (1DT) with bulk parameterization. In this model, the cloud is modeled as a circular air column with a time-dependent radius in an environment at rest. All dynamical equations are formulated in a one-dimensional space based on Asai and Kasahara (1967). The effect of downward compensation in the environment is not considered.

The equation of the vertical component of velocity in a cylindrical coordinate may be written as

$$\frac{\partial w}{\partial t} = w\frac{\partial w}{\partial z} - \frac{2\alpha^2}{a} w|w| + \frac{2}{a}\tilde{u}_a(w - \tilde{w}_a) + g\frac{T_v - T_{v0}}{T_{v0}} - g(Q_c + Q_r + Q_G) \quad (1)$$

The first term on the right-hand side of Eq. (1) represents the vertical advection, the second term the lateral eddy exchange, the third term the dynamic entertainment that is required to satisfy the mass continuity between the cloud and the environment, the fourth term the buoyancy, and the last term the drag force that is assumed to be provided by the weight of cloud droplets, raindrops, and hail. In this equation, $\tilde{u}_a$ which is the value of u_a at r=a, is determined by the following equation with the boundary condition that w=0 at z=0,

$$\frac{2}{a}\tilde{u}_a + \frac{1}{\rho_{a0}}\frac{\partial}{\partial z}(\rho_{a0}\overline{w}) = 0 \quad (2)$$

In DOT model, nine microphysical processes have been parameterized with four water substances including water vapor, cloud droplet, raindrop and hail as shown in Figure 1. The equations of the microphysical process simulated in DOT model are presented in Table 1 (Javanmard, 1995).

2.2 Lin et al. Model (1983)

It is a two-dimensional, time-dependent cloud model which is used to simulate a moderate intensity thunderstorm. In this model six forms of water substances (water vapor, cloud water, cloud ice, rain, snow and hail/graupel) are simulated that are presented in Table 2 and 3 microphysical processes are considered as shown in Figure 2. The model utilizes the "bulk water" microphysical parameterization to represent the precipitation fields which are all assumed to follow exponential size distribution functions. Autoconversion concepts are used to parameterize the collision-coalescence and collision-aggregation processes. Accretion processes involving the various forms of liquid and solid hydrometeors are simulated in this model. The transformation of cloud ice to snow through autoconversion (aggregation) and Bergeron processes and the subsequent accretional growth or

aggregation to form hail are simulated too. Hail is also produced by various contact mechanisms and via probabilistic freezing of raindrops. Evaporation (sublimation) is considered for all precipitation particles outside the cloud. The melting of hail and snow are included in the model. Wet and dry growth of hail and shedding of rain from hail are simulated as well (Lin *et al*., 1983).

2.3 Developed Lin et al. Microphysical Processes (DLMP) Model

In DLMP model, dynamic and thermodynamic equations are based on DOT model in which cloud ice and snow are added and its microphysics is based on Lin *et al*. model.

The equations of vertical velocity, temperature, continuity for water vapor, cloud droplets, cloud ice, raindrops, snow, and hail particles, respectively, are given as follows:

$$\frac{\partial w}{\partial t} = -w\frac{\partial w}{\partial z} - \frac{2\alpha^2}{a}w|w| + \frac{2}{a}\tilde{u}_a(w - \tilde{w}_a) + g\frac{T_v - T_{v0}}{T_{v0}} - g(Q_c + Q_r + Q_G + Q_i + Q_s) \quad (3)$$

$$\frac{\partial T}{\partial t} = -w\frac{\partial T}{\partial Z} + \frac{2\alpha^2}{a}|W|(T_0 - T) + \frac{2}{a}\tilde{u}_a\left(T - \tilde{T}_a\right) + \left(\frac{L_v}{C_P}\right)(P_{CON} - P_{CEVP} - P_{REVP}) + \left(\frac{L_s}{C_P}\right)(-P_{IEVP} + P_{NUA} +$$

$$P_{IDEP} - P_{SSUB} - P_{GSUB} + P_{SDEP}) + \left(\frac{L_f}{C_P}\right)(-P_{IMLT} + P_{SFW} + P_{IACRS} + P_{SACRS} + P_{SACW} - P_{SMLT} + P_{GFR} +$$

$$P_{GACW} + P_{GACR} + P_{SACRG} + P_{IACRG} - P_{GMLT} + P_{NUH} + P_{NUF}) \quad (4)$$

$$\frac{\partial Q_v}{\partial t} = -w\frac{\partial Q_v}{\partial Z} + \frac{2\alpha^2}{a}|w|(Q_{v0} - Q_v) + \frac{2}{a}\tilde{u}_a\left(Q_v - \tilde{Q}_{va}\right) + P_v \quad (5)$$

$$\frac{\partial Q_c}{\partial t} = -w\frac{\partial Q_c}{\partial Z} - \frac{2\alpha^2}{a}|w|(Q_c) + \frac{2}{a}\tilde{u}_a\left(Q_c - \tilde{Q}_{ca}\right) + P_c \quad (6)$$

$$\frac{\partial Q_r}{\partial t} = -w\frac{\partial Q_r}{\partial Z} + w\frac{\partial V_W}{\partial Z} - \frac{2\alpha^2}{a}|w|(Q_r) + \frac{2}{a}\tilde{u}_a\left(Q_r - \tilde{Q}_{ra}\right) + P_r \quad (7)$$

$$\frac{\partial Q_i}{\partial t} = -w\frac{\partial Q_i}{\partial Z} - \frac{2\alpha^2}{a}|w|(Q_i) + \frac{2}{a}\tilde{u}_a\left(Q_i - \tilde{Q}_{ia}\right) + P_i \quad (8)$$

$$\frac{\partial Q_s}{\partial t} = -w\frac{\partial Q_s}{\partial Z} + w\frac{\partial V_s}{\partial Z} - \frac{2\alpha^2}{a}|w|(Q_s) + \frac{2}{a}\tilde{u}_a\left(Q_s - \tilde{Q}_{sa}\right) + P_s \quad (9)$$

$$\frac{\partial Q_G}{\partial t} = -w\frac{\partial Q_G}{\partial Z} + w\frac{\partial V_G}{\partial Z} - \frac{2\alpha^2}{a}|w|(Q_G) + \frac{2}{a}\tilde{u}_a\left(Q_G - \tilde{Q}_G\right) + P_G \quad (10)$$

where V_w ,V_s , and V_G are terminal velocity of raindrop, snow, and hail, respectively, and P_v, P_c, P_r, P_i, P_s, and P_G are rate of production of water vapor, cloud droplet, raindrop, cloud ice, snow, and hail/graupel as follows:

$$V_w = \frac{a\Gamma(4+b)}{6\lambda_R^b}\left(\frac{\rho_0}{\rho}\right)^{1/2} \quad (11)$$

$$V_s = \frac{C_s\Gamma(D+4)}{6\lambda_S^D}\left(\frac{\rho_0}{\rho}\right)^{1/2} \quad (12)$$

$$V_G = \frac{\Gamma(4.5)}{6\lambda_I^{0.5}}\left(\frac{4g\rho_I}{3C_D\rho}\right)^{1/2} \quad (13)$$

$$P_v = P_{CEVP} + P_{REVP} + P_{SSUB} + P_{GSUB} + P_{IEVP} - (P_{CON} + P_{SDEP} + P_{IDEP} + P_{NUA}) \quad (14)$$

$$P_c = P_{CON} + P_{IMLT} - (P_{RAUT} + P_{RACW} + P_{NUH} + P_{NUF} + P_{CEVP} + P_{SFW} + P_{GACW} + P_{SACW}) \quad (15)$$

$$P_i = P_{NUH} + P_{NUF} + P_{NUA} + P_{IDEP} - (P_{RACIS} + P_{SAUT} + P_{SACI} + P_{SFI} + P_{RACIG} + P_{IEVP} + P_{IMLT}) \quad (16)$$

$$P_r = P_{RAUT} + P_{RACW} + P_{SACW} + P_{GACW} + P_{SMLT} + P_{GMLT} - (P_{REVP} + P_{IACRS} + P_{SACRS} + P_{IACRG} + P_{GFR} + P_{SACRG} + P_{GACR}) \quad (17)$$

$$P_s = P_{SAUT} + P_{SACI} + P_{SACW} + P_{SFW} + P_{SFI} + P_{RACIS} + P_{IACRS} + P_{SACRS} + P_{SDEP} - (P_{RACS} + P_{GACS} + P_{GAUT} + P_{SSUB} + P_{SMLT}) \quad (18)$$

$$P_G = P_{RACIG} + P_{RACS} + P_{GAUT} + P_{IACRG} + P_{GFR} + P_{SACRG} + P_{GDRY} + P_{GWET} + P_{GACS} - (P_{GSUB} + P_{GMLT}) \quad (19)$$

3. Numerical Calculation Method in DLMP Model

The numerical calculation method in DLMP model is based on DOT model. This is a coupled, one-dimensional cloud model with balk microphysical parameterization. The space increment along the vertical direction (Δz) is 250 m and the time increment (Δt) is 5 s. The prognostic equations of vertical velocity (W), temperature (T), mixing ratios of water vapor (Q_v), mixing ratios of cloud droplets (Q_c), mixing ratios of cloud ice (Q_i), mixing ratios of rain water (Q_r), mixing ratios of snow (Q_s), and mixing ratios of hail (Q_G) are solved by a finite difference method. The numerical method used is forward difference. All spatial derivatives, except for those in the advection terms of the equations, have been calculated from centered difference.

W, T, Q_v, Q_c, Q_i, Q_r, Q_s and Q_G are zero at ground surface and at the top of the atmosphere they are assumed to be 15 km from the surface. Initial motion in atmosphere starts at a distance of 2Km above the surface by a small updraft movement as follows:

$$w_{t=0} = \Delta w(\frac{z}{z_o})(2 - \frac{z}{z_o}) \quad (20)$$

Where $\Delta w = 1 m/s$ and z_o=1km.

Temperature at ground surface is 25℃ and its lapse rate is 6.3℃/km and more than 10km is constant. Relative humidity at ground surface is 100% and it decreases 5% per kilometer.

The calculation procedure is

1) $\tilde{u}_a$ is calculated from w using Eq. (2);

2) V_W, V_S, and V_G are calculated using Eqs. (11) to (13);

3) The quantities of, W, T, Q_v, Q_c, Q_i, Q_r, Q_s and Q_G are calculated considering the dynamical terms in the prognostic Eqs. (3) through (10);

4) In this step, Q_{vs} and Q_{is} which are saturation mixing ratios over water and ice, respectively, as a function of temperature are given as follows:

$$Q_{vs} = 3.8P^{-1}10\frac{7.5(T-273)}{T-6} \quad (21)$$

$$Q_{is} = 3.8P^{-1}10\frac{9.5(T-273)}{T-8} \quad (22)$$

Where P is the atmospheric pressure. These calculations include different states of $T \lesseqgtr 273$ $Q_V \lesseqgtr Q_{VS}$ $Q_V \lesseqgtr Q_{iS}$, $Q_{is}<Q_V<Q_{VS}$, $Q_r \lesseqgtr 0$ $Q_G \lesseqgtr 0$ and $Q_s \lesseqgtr 0$. Sometimes, two or three physical processes occur simultaneously. For example, in unsaturated air, evaporation of cloud droplet, rain drops, cloud ice, snow, and hail occurs simultaneously. In another case, it is assumed that, at first, cloud droplets would be evaporated. If the air is still unsaturated, rain, cloud ice, snow, and hail will be evaporated. The condition that the whole evaporation should not exceed water vapor amount should always be satisfied.

5) In the next step, the values of T, Q_v, Q_c Q_i Q_r Q_s and Q_G are calculated considering the sources and sinks terms ($P_1 \ldots P_{32}$). One-time increment calculation should be completed by performing steps (1) through (5).

The programming language used for DLMP model is Fortran and Tecplot and Excel software is used to draw model outputs.

4. Results

In this section, we will compare the output graphs of DOT and DLMP models including the contours of mixing ratios of rain water, snow, rainfall intensity, temperature difference between cloud and environment, vertical velocity and the graphs of source, sink terms and rainfall intensity at ground surface amounts versus time.

4.1 Mixing ratio of rainwater (Q_r)

The contours of rain water mixing ratio versus height and time are shown in Figures 3 a & b, in which the maximum value of rain water mixing ratio in DLMP model is 5.9 gkg^{-1} and its minimum value is 0.4 gkg^{-1}. Comparison of Figures 3 a & b shows that the maximum and minimum values have increased 1.9 gkg^{-1} and 0.13 gkg^{-1}, respectively, compared to DOT model, and the raindrop has appeared 2.5 km above.

We have studied these differences in view of source and sink terms. From Figures 4 a & b, it could be concluded that the rain production source terms in DLMP model are more than DOT model. The most effective terms in DLMP model are P_{GACW} and P_{RACW} (accretion of cloud water by hail and accretion of cloud water by rain) and in DOT model is P_2 (conversion of cloud droplets to rain water). Considering Figures 5 a & b, we have observed that the number of sink terms in DLMP model is fewer than that of DOT model, and the most effective term in DLMP model is P_{IACRG} (accretion of rain water by cloud ice to produce hail) and in DOT model is P_2 (glaciation of raindrops to produce hail).

4.2 Mixing Ratio of Snow (Q_S) in DLMP Model

The contours of snow mixing ratio versus height and time are shown in Figures 6 a & b, in which the maximum and minimum values of snow mixing ratio in DLMP model are 0.52 gkg^{-1} and 0.032 gkg^{-1}, respectively, and has reached 11.2 km.

We studied snow source and sink terms in Figures 7 and 8. The most effective source term in DLMP model is P_{SACW} (accretion of cloud water by snow) and the most effective sink term is P_{RACSG} (accretion of snow by rain water to produce hail).

4.3 Rainfall Intensity (PR)

The contours of rainfall intensity versus height and time are shown in Figures 9 a & b, in which the maximum value of rainfall intensity in DLMP model is 103.3 mm/h and it is at time increment of 42-48 min and at heights of 500 m to 2.5 km. Comparison of Figures 9 a & b, shows that the maximum value is 78.1mm/h higher in DLMP model than the one in DOT model in which it occurs at time increment of 40-58 minutes and between 400 m - 3km.

This difference is due to the existence of more terms for transformation of other water substances into rain in DLMP model. The regions where PR is negative, there are updraft and evaporation, so precipitation is little. If PR is positive, there is downdraft and we observe considerable precipitation.

4.4 Difference of Temperature between Cloud and Environment (TT)

We define TT quantity as a temperature difference between cloud and environment. If TT is positive in a region, it is due to cloud temperature enhancement from condensation, deposition and freezing. Then, latent heat is released to cloud environment and, therefore, we expect cloud and precipitation in that region. Moreover, if TT becomes negative in the region, it means that cloud temperature has decreased due to evaporation, sublimation, snow and hail melting; therefore, cloud and precipitation would not be expected.

Comparison of Figures 9 a & b, shows that the maximum value of TT is 4.09℃ in DLMP model and it is 3.95℃ in DOT model. This temperature difference between the two models (0.14℃) is due to the inclusion of more parameters in DLMP model which will cause more precipitation, and, therefore, release more heat to environment in DLMP model. Thus, it causes higher temperature difference between cloud and environment.

4.5 Vertical Velocity Component (w)

The contours of vertical velocity component in DOT and DLMP models have been compared in Figure 10, in which the maximum value of w in DLMP model is 23 m/s, which is 3m/s greater than its value in DOT model. If the temperature difference between the cloud and environment is greater, buoyancy force will be more (the fourth term in Eq. 3), and, therefore, w will be greater. Comparison of Figures 9 and 10 shows that the maximum

value of TT in DLMP model is about 0.14℃ more than that of DOT model, which causes the vertical velocity maximum to increase about 3m/s.

4.6 Rainfall Intensity at Ground Surface (GPR)

GPR quantity is the rate of rainfall intensity (PR) at ground surface and Figures 11 a & b show the temporal variation of GPR in DOT and DLMP models. Comparison of Figures 11 a & b shows that the maximum value of GPR in DLMP model is 114mm/h in 52 min. This quantity, in DOT model, is about 34mm/h in 56 min. In DLMP model, precipitation started in 30 minutes and ended in 81 min (a time period of 51 min), and in DOT model, it started in 22 and ended in 85 min (a time period of 63 min).

5. Discussion and Conclusion

In this paper, DOT model has been improved to develop DLMP model with respect to microphysical processes and the products of these two models have been compared. Both models were run in the same environmental and initial conditions, but more complex microphysical parameterization was applied in DLMP model. In comparison with DOT model, the mixing ratio of rain water increased when more source and sink terms were inserted. The snow mixing ratio was derived in DLMP model, which did not exist in DOT model. The rain mixing ratio and terminal velocity of rain enhanced in the regions where air density was low, so rainfall intensity at ground surface increased. In DLMP model, the number of exothermic processes, such as condensation, deposition, and freezing, was greater than that of DOT model, which led to the release of more latent heat in cloud and enhancement of updraft vertical velocity.

Since microphysical processes which caused downdraft in DLMP model enhanced, the estimated maximum value of PR increased.

The maximum value of GPR in DLMP model was nearer to the experimental observations. For example, Morin *et al*. (2006) studied spatial rainfall patterns associated with air mass thunderstorm events in hydrological model and showed that maximum rainfall intensity reached about 170mm/h in 70 minutes. Takahashi and Kawano (1997) examined the effect of different microphysical treatments on rain evolution and precipitation processes using a deep, two-dimensional rainband model. The maximum value of rainfall intensity reached 126mm/h in 30 minutes and 86.7mm/h in 60 minutes.

The convective cloud model based on microphysics of DLMP model simulates precipitation process and pattern at ground surface more accurately because convective and thunderstorm clouds naturally produce high rainfall intensity in a short time.

Since precipitation monitoring is important in environmental studies and hazard risk reduction, researchers are interested in modeling high resolution temporal and spatial distribution of rainfall using advanced technologies including space-based systems (satellites) (Javanmard *et al*., 2009; 2011).

References

Asai, T. & Kasahara, A. (1967). A Theoretical study of the compensating downward motions associated with cumulus clouds. *J. Atmos. Sci.*, 24, 487-496. http://dx.doi.org/10.1175/1520-0469(1967)024<0487:ATSOTC>2.0.CO;2

Danielsen, E. F, Black, R. & Morris, D. A. (1972). Hail growth by stochastic collection in a cumulus model. *J. Atmos. Sci.*, 29, 135- 155. http://dx.doi.org/10.1175/1520-0469(1972)029<0135:HGBSCI>2.0.CO;2

Jamali, J. B. & Javanmard, S. (2004). Improvement of microphysical and dynamical parameterization of Ogura and Takahashi's numerical thunderstorm model, IR. *J. Sci. Tech.*, 28(B5), 595-604.

Javanmard, S. & Jamali, J. B. (2003). Parameterization of microphysical and dynamical processes of rainfall in thunderstorm cloud model, IR. *J. Phys.*, 3(3), 185-198.

Javanmard, S. (1995). Improvement Ogura- Takahashi's numerical thunderstorm model, M. S. Thesis, Faculty of Science, Kyushu Univ. Japan.

Javanmard, S. Yatagai, A. Nodzu, M. *et al*. (2010). Comparing high resolution gridded precipitation data with satellite rainfall estimates of TRMM 3B42 over Iran. *Adv. in Geosci.*, 25, 119-125. http://dx.doi.org/10.5194/adgeo-25-119-2010

Javanmard, S., Jamali, J. B., & Rajaei, V. M. (2008). Numerical study of microphysical parameterization in one-dimensional thunderstorm cloud model. Iranian Annual Physics Conference, Kashan.

Javanmard, S., Yagagai, A., Nodzu, M. I., *et al*. (2009). Improvement of daily gridded precipitation data using synoptic observation data over Iran, Jpn. Meteorol. Soc., Spring meeting, Tsukuba, 28-31 May 2009.

Koenig, L. R. & Murray, F. W. (1976). Ice-bearing cumulus cloud evolution: Numerical simulation and general comparison against observation. *J. Appl. Met.*, 15, 747- 762. http://dx.doi.org/10.1175/1520-0450(1976)015<0747:IBCCEN>2.0.CO;2

Lin, Y. L., Farely, R. D. & Orville, H. D. (1983). Bulk parameterization of snow field in a cloud model. *J.Climate Appl. Meteor.*, 23, 1065. http://dx.doi.org/10.1175/1520-0450(1983)022<1065:BPOTSF>2.0.CO;2

Marshall, J. S. & Palmer, W. M. (1948). The distribution of raindrops with size. *J. Meteor.*, 5, 165-166. http://dx.doi.org/10.1175/1520-0469(1948)005<0165:TDORWS>2.0.CO;2

Morin, E., Goodrich, D. C., Moddox, R. A., *et al*. (2006). Spatial Patterns in Thunderstorm Rainfall Events and their Coupling with Watershed Hydrological Response. *Adv. water Res.*, 29, 843.

Ogura, Y. & Takahashi, T. (1971). Numerical simulation of the life cycle of a thunderstorm cell, Mon. *Wea. Rev.*, 99, 895-911. http://dx.doi.org/10.1175/1520-0493(1971)099<0895:NSOTLC>2.3.CO;2

Orville, H. D. (1996). A review of cloud modeling in weather modification. *Bull. Amer. Meteor. Soci.*, 77, 1535-1555. http://dx.doi.org/10.1175/1520-0477(1996)077<1535:AROCMI>2.0.CO;2

Rajaei, V. M. (1387). Master Thesis, Faculty of Science, Zanjan Univ., Iran.

Simpson, J. (1970). Cumulus cloud modification: Progress and prospects. *A century of wea. Prog*., 143-155.

Takahashi, T. & Kawano, T. (1997). Numerical sensitivity study of rainband precipitation and evolution. *J. Atoms. Sci.*, 55, 57-87. http://dx.doi.org/10.1175/1520-0469(1998)055<0057:NSSORP>2.0.CO;2

Table 1. Equations of microphysical process simulated in DOT model (Javanmard, 1995)

Microphysical processes	Notations	Equations
Rate of condensation	P_1	$P1 = \frac{Q_V - Q_{VS}}{\Delta t}$
Rate of conversion of cloud droplets to rain water	P_2	$P2 = k_1(Q_C - Q_{CO}) + k_2 Q_C Q_r^{0,875}$
Rate of glaciations	P_3	$P_3 = 20\pi^2 BN_{OR}(\frac{\rho_W}{\rho})\lambda_R^{-7}\{\exp[A(T-T_O)]-1\}$
Rate of sublimation	P_4	$P_3 = 20\pi^2 BN_{OR}(\frac{\rho_W}{\rho})\lambda_R^{-7}\{\exp[A(T-T_O)]-1\}$
Rate of melting	P_5	$P_5 = 2.27\times10^{-6}C(T-273)(\rho_a Q_G)0.525 f_o^{-0.420}$
Rate of evaporation of cloud droplets	P_6	$P_6 = \frac{-1}{\rho_a}\frac{(\frac{Q_V}{Q_{VS}}-1)(\rho_a Q_r)^{0.525}}{5.4\times10^5 + \frac{0.41\times10^7}{e_{WS}}}$
Rate of evaporation of raindrops	P_7	$P_7 = \frac{-1}{\rho_a}\frac{(\frac{Q_V}{Q_{VS}}-1)C_W(\rho_a Q_r)^{0.525}}{5.4\times10^5 + \frac{0.41\times10^7}{e_{WS}}}$
Rate of evaporation of hail	P_8	$P_7 = \frac{-1}{\rho_a}\frac{(\frac{Q_V}{Q_{VS}}-1)C_W(\rho_a Q_r)^{0.525}}{5.4\times10^5 + \frac{0.41\times10^7}{e_{WS}}}$
Rate of evaporation of melting hail	P_9	$P_9 = \frac{-1}{\rho_a}\frac{(\frac{Q_V}{Q_{VS}}-1)C(\rho_a Q_C)^{0.525} f_o^{-0.42}}{5.4\times10^5 + \frac{0.41\times10^7}{e_{WS}}}$

Table 2. Microphysical processes in Lin *et al*. model (1983)

Notation	Description
P_{CON}	Condensation
P_{IMLT}	Melting of cloud ice to form cloud water, $T \geq T_O$
P_{IACRS}/P_{IACRG}	Accretion of rain by cloud ice produces snow or graupel
$P_{NUA}/P_{NUH}/P_{HUF}$	Nucleation for producing water vapor to ice nuclei
P_{RAUT}	Autoconversion of cloud water to form rain
P_{CEVP}	Evaporation of cloud water
P_{REVP}	Evaporation of rain
P_{RACW}	Accretion of cloud water by rain
P_{RACIS}/P_{RACIG}	Accretion of cloud ice by rain produces snow or graupel
P_{IACRS}/P_{IACRG}	Accretion of rain by cloud ice produces snow or graupel
P_{SACW}	Accretion of cloud water by snow
P_{SACRS}/P_{SACRG}	Accretion of rain by snow produces snow or graupel
P_{IDEP}	Deposition growth of cloud ice
P_{SACI}	Accretion of cloud ice by snow
P_{SAUT}	Autoconversion of cloud ice to form snow
P_{SFW}	Bergeron process (deposition and riming)- transfer of cloud water to form snow
P_{SFI}	Transformation of cloud ice to snow through Bergeron process embryos
P_{SDEP}	Deposition growth of snow
P_{SSUB}	Sublimation of snow
P_{SMLT}	Melting of snow to form rain
P_{GAUT}	Autoconversion of snow to form graupel
P_{GFR}	Probabilistic freezing of rain to form graupel
P_{GACW}	Accretion of cloud water by graupel
P_{GACR}	Accretion of rain by graupel
P_{GACS}	Accretion of snow by graupel
P_{GMLT}	Melting of graupel to form rain
P_{GSUB}	Sublimation of graupel
P_{IEVP}	Evaporation of cloud ice
P_{GDRY}/P_{GWET}	Dry/ wet growth of graupel
P_{RACS}	Accretion of snow by rain

Table 3. List of Symbols

Notation	Description
A	Radius of cloud column
α^2	Lateral mixing parameter
a	Constant in empirical formula for V_W
A	Constant in Bigg's freezing
b	Constant in empirical formula for V_W
B	Constant in raindrop freezing equation
C	Ventilation coefficient for hail particles
C_O	Constant in rate of autoconversion
C_D	Drag coefficient for hailstone
C_P	Specific heat at constant pressure
C_W	Ventilation of coefficient for raindrop
C_S	Constant in empirical formula for V_S
D	Constant in empirical formula for V_S
Δt	Time step of numerical integration
e_{is}	Saturation vapor pressure over ice
e_{ws}	Saturation vapor pressure over water
f_0	Ventilation coefficient for particles
G	Acceleration of gravity
K_1	Constant in Kessler equation
K_2	Constant in Kessler equation
L_f	Latent heat of freezing
L_s	Latent heat of sublimation
L_v	Latent heat of evaporation
N_{OR}	Number of raindrops per unit diameter
λ_I	Slope parameter in hail size distribution
λ_R	Slope parameter in rain size distribution
λ_S	Slope parameter in snow size distribution
P	Environmental atmospheric pressure
P_C	Rate of production of cloud droplet
P_i	Rate of production of cloud ice
P_G	Rate of production of hail
P_r	Rate of production of rain
P_S	Rate of production of snow
P_V	Rate of production of water vapor
Q_C	Mixing ratio of cloud droplet
Q_{CO}	Cloud water mixing ratio in environment
$\tilde{Q}ca$	Mean value of cloud water mixing ratio at r=a
Q_i	Mixing ratio of cloud ice
Q_{io}	Cloud ice mixing ratio in environment

$\tilde{Q}ia$	Mean value of cloud ice mixing ratio at r=a
Q_G	Mixing ratio of hail
Q_{GO}	Hail mixing ratio in environment
$\tilde{Q}_{Ga}$	Mean value of hail mixing ratio at r=a
Q_r	Mixing ratio of rain drop
Q_{ro}	Rain drop mixing ratio at environment
$\tilde{Q}_{ra}$	Mean value of rain drop mixing ratio at r=a
Q_S	Mixing ratio of snow
Q_{SO}	Snow mixing ratio in environment
$\tilde{Q}_{sa}$	Mean value of snow mixing ratio at r=a
Q_V	Mixing ratio of water vapor
Q_{VO}	Water vapor mixing ratio in environment
$\tilde{Q}_{va}$	Mean value of water vapor mixing ratio at r=a
ρ_{ao}	Air density at environment
ρ_a	Density of dry air
ρ_i	Density of hail
ρ_w	Density of water
ρ_o	Surface air density
T	Cloud temperature
T_0	Melting temperature
T_V	Virtual temperature
T_{VO}	Virtual temperature in environment
u_a	Radial velocity
$\tilde{u}_a$	Mean value of u_a at r=a
V_G	Terminal velocity of hail
V_S	Terminal velocity of snow
V_W	Terminal velocity of rain drops
W	Vertical component of velocity
$\tilde{w}_a$	Mean value of vertical velocity at r=a

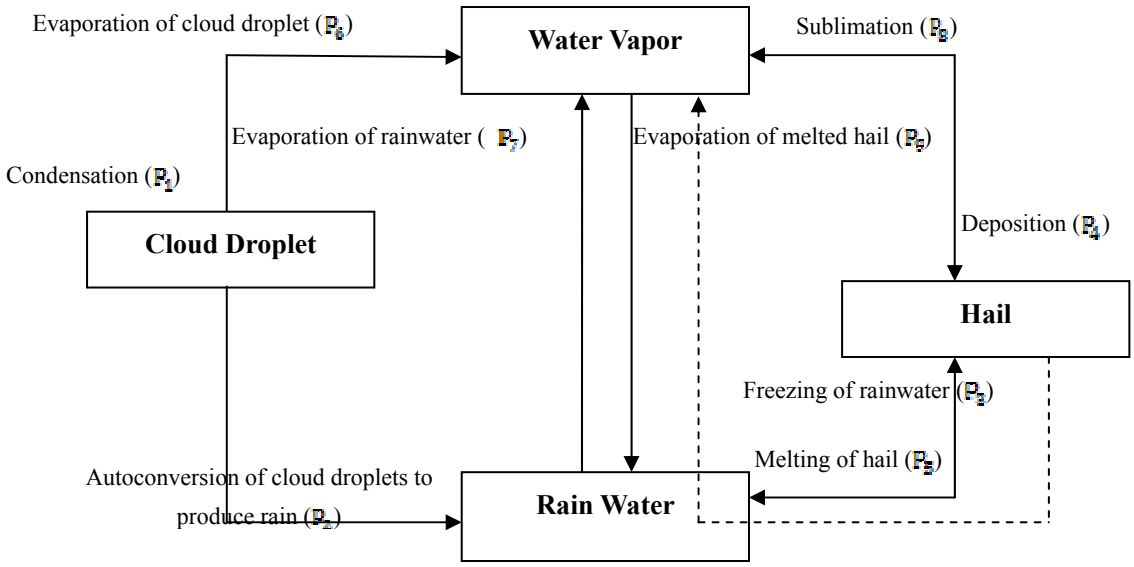

Figure 1. Microphysical processes based on DOT model (Javanmard, 1995)

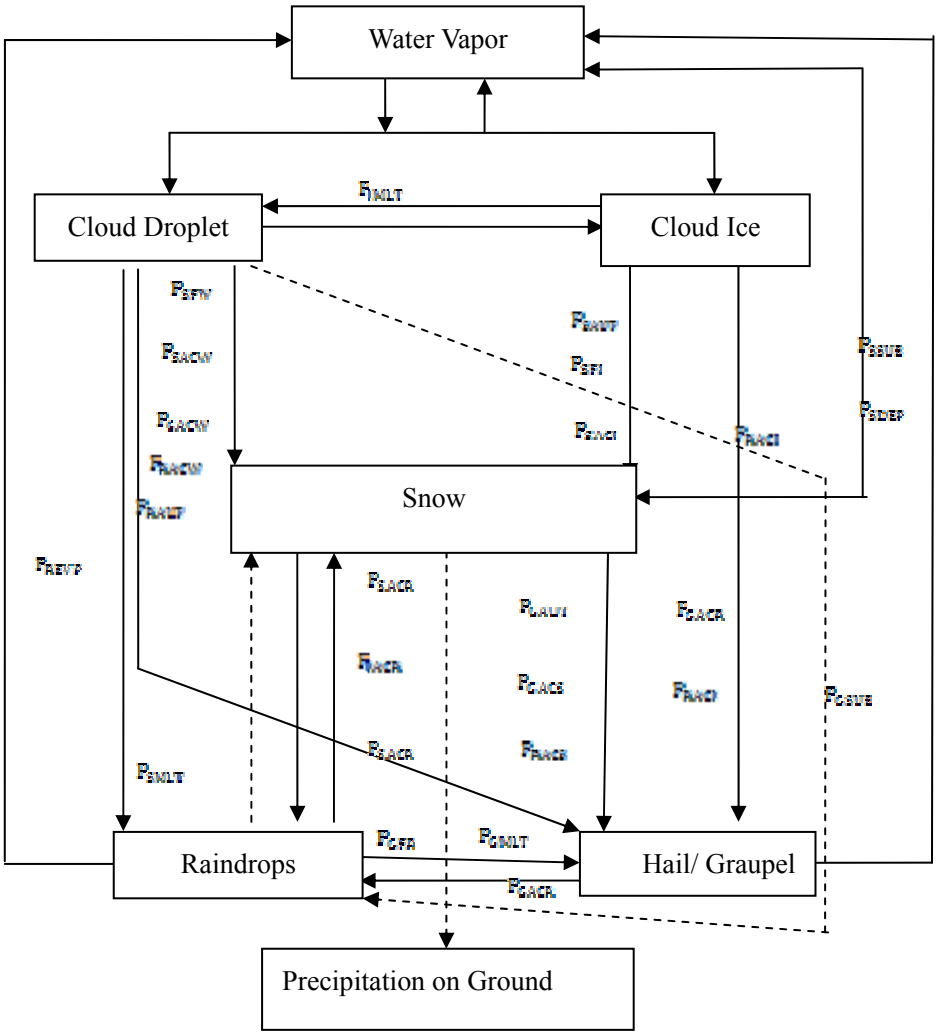

Figure 2. Microphysical processes in Lin *et al*. model (1983)

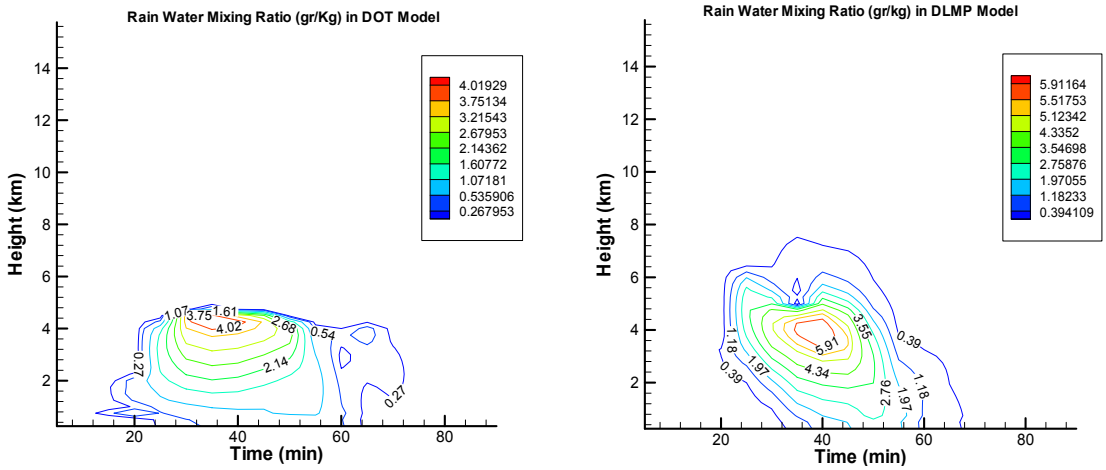

(a) (b)

Figure 3. Comparison of the rain water mixing ratio changes with height and time in (a) DOT Model and (b) DLMP model

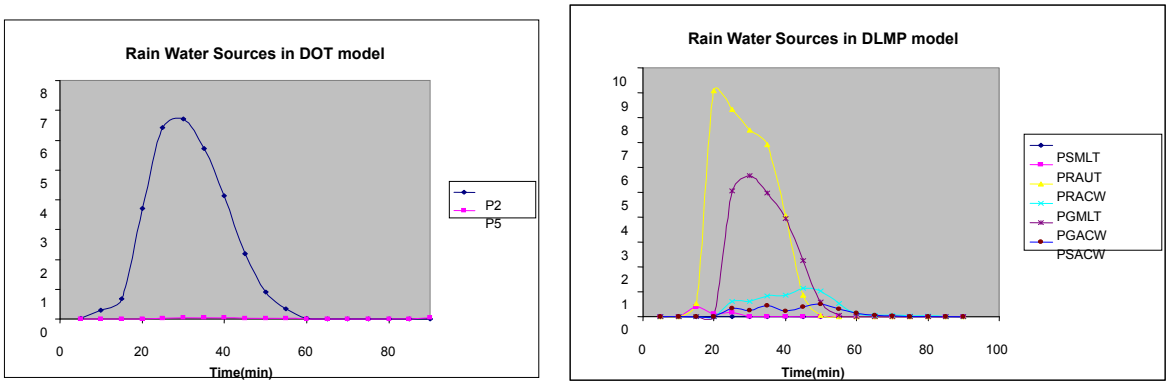

(a) (b)

Figure 4. Comparison of the rain producing source terms in (a) DOT Model and (b) DLMP model

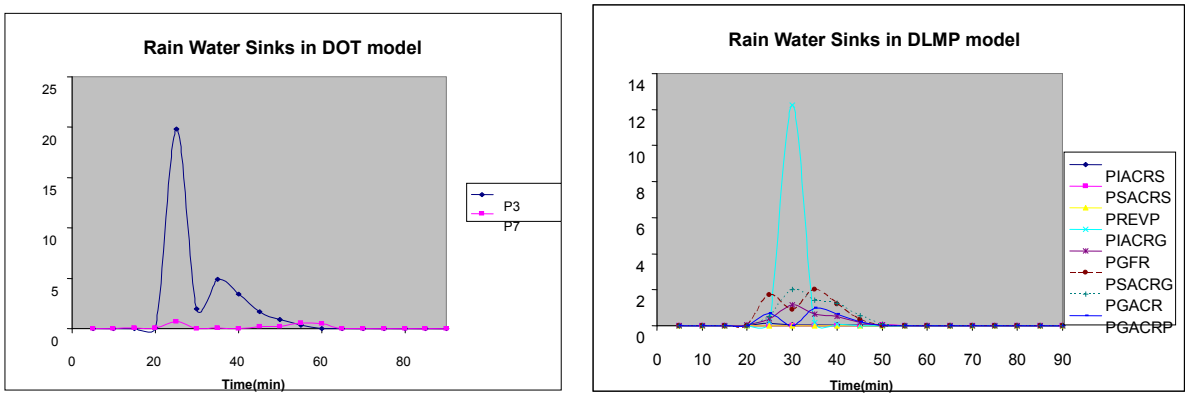

(a) (b)

Figure 5. Comparison of the rain sink terms in (a) DOT model and (b) DLMP model

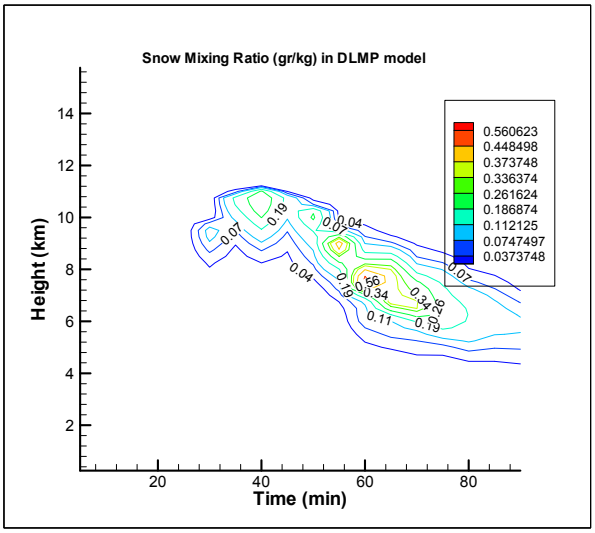

Figure 6. Snow mixing ratio changes to height and time in DLMP model

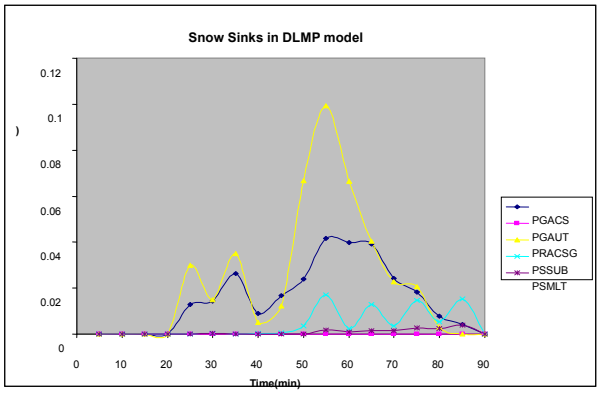

Figure 7. Snow sink terms in DLMP the model

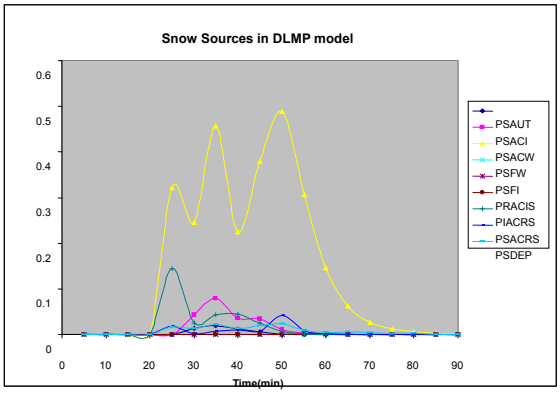

Figure 8. Snow producing source terms in DLMP model

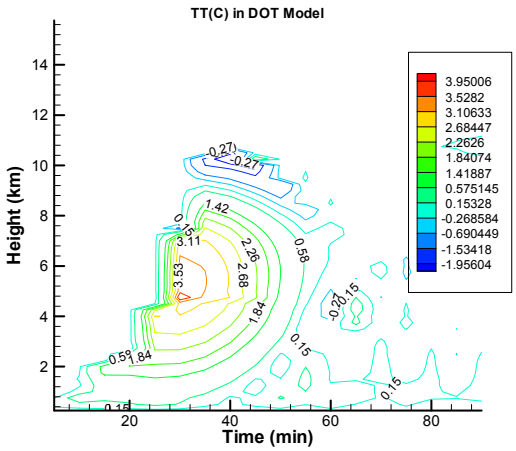

(a)

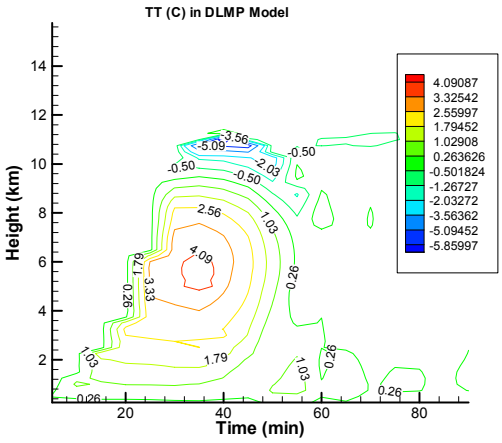

(b)

Figure 9. Comparison of the temperature difference between cloud and environment (℃) in (a) DOT Model and (b) DLMP model

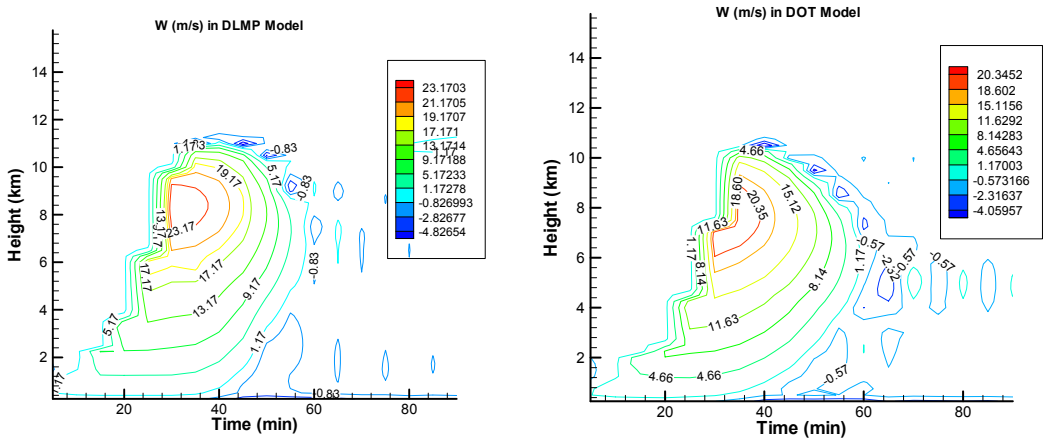

(a) (b)

Figure 10. Comparison of vertical velocity (m/s) in (a) DOT Model and (b) DLMP model

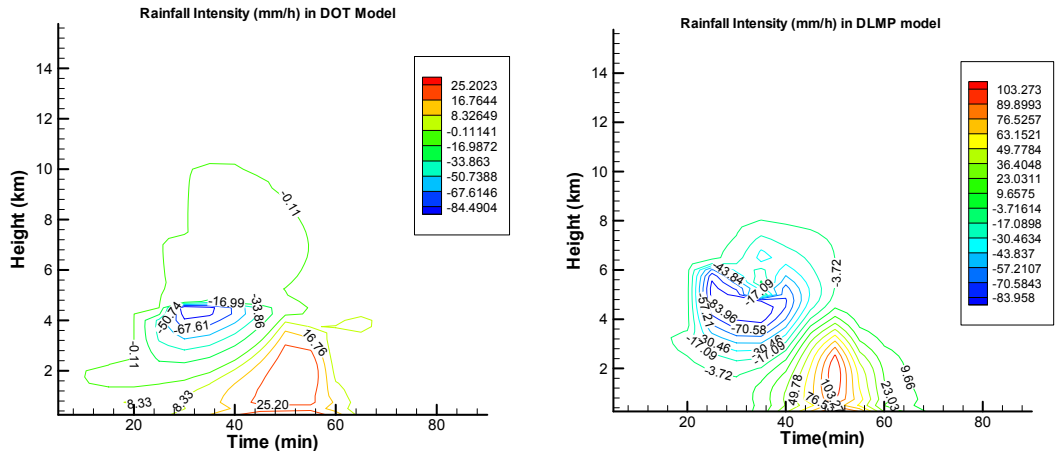

(a) (b)

Figure 11. Comparison of rainfall intensity changes with height and time (gr/kg) in (a) DOT model and (b) DLMP model

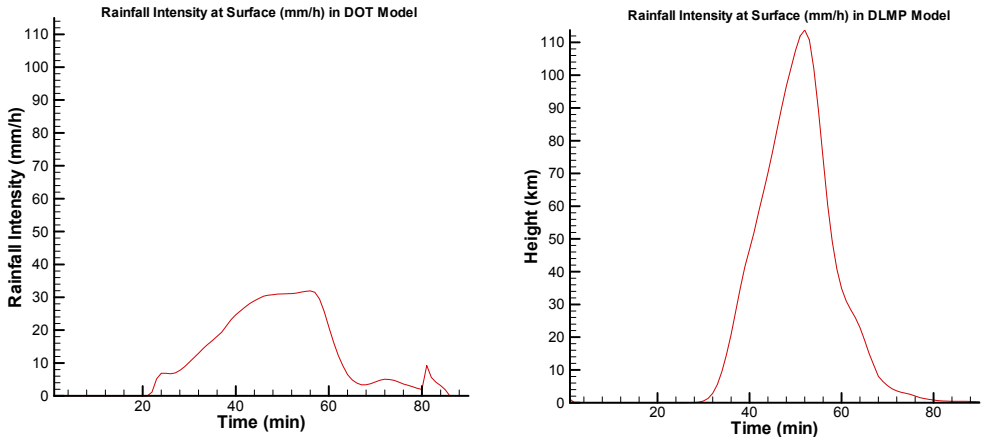

(a) (b)

Figure 12. Comparison of rainfall intensity at ground surface (mm/h) in (a) DOT model and (b) DLMP model